

Exact solution for quantum strong long-range models via a generalized Hubbard-Stratonovich transformation

Juan Román-Roche , Víctor Herráiz-López , and David Zueco 

Instituto de Nanociencia y Materiales de Aragón (INMA), CSIC-Universidad de Zaragoza, Zaragoza 50009, Spain and Departamento de Física de la Materia Condensada, Universidad de Zaragoza, Zaragoza 50009, Spain



(Received 5 June 2023; accepted 4 October 2023; published 18 October 2023)

We present an exact analytical solution for quantum *strong* long-range models in the canonical ensemble by extending the classical solution proposed in Campa *et al.* [*J. Phys. A: Math. Gen.* **36**, 6897 (2003)]. Specifically, we utilize the equivalence between generalized Dicke models and interacting quantum models as a generalization of the Hubbard-Stratonovich transformation. To demonstrate our method, we apply it to the Ising chain in transverse field and discuss its potential application to other models, such as the Fermi-Hubbard model, combined short- and long-range models, and models with antiferromagnetic interactions. Our findings indicate that the critical behavior of a model is independent of the range of interactions, within the strong long-range regime, and the dimensionality of the model. Moreover, we show that the order-parameter expression is equivalent to that provided by mean-field theory, thus confirming the exactness of the latter. Finally, we examine the algebraic decay of correlations and characterize its dependence on the range of interactions in the full phase diagram.

DOI: [10.1103/PhysRevB.108.165130](https://doi.org/10.1103/PhysRevB.108.165130)

I. INTRODUCTION

Long-range systems are those in which two-body interactions decay as a power law at large distances. They are ubiquitous in nature, with some examples given by dipolar, Coulomb, or van der Waals interactions. Recent experimental advances in atomic, molecular, and optical systems have led to a resurgence of interest in long-range models [1–4]. In these experiments, the effective interactions between spins are often long ranged and tunable, renewing the need for a comprehensive understanding of long-range systems. Although less studied than their short-ranged counterparts, there are already some rigorous and numerical results available [5–9]. Some equilibrium and dynamical properties have been discussed in comparison with short-range systems. Notable examples are the existence (or absence) of an area law of entanglement [10–13], the algebraic decay of two-point correlators out of criticality [14–16], the spreading of correlations [17], the existence of Majorana modes [18], and topological properties [19].

In these examples, the phenomenology can be understood within a (sub)classification in terms of the range of interactions they exhibit. To fix notation and ideas, let us introduce this classification with the models considered in this paper: quantum long-range models in an N -site lattice with a coupling of the form

$$\mathcal{H}_c = - \sum_{ij}^N J_{ij} \mathcal{C}_i \mathcal{C}_j, \quad (1)$$

where \mathcal{C}_i is a local Hermitian operator acting on site i . We consider models with power-law decaying interactions $J_{ij} = \Gamma \tilde{J}(\mathbf{r}_{ij}) / \tilde{N}$,

$$\tilde{J}(\mathbf{r}_{ij}) = \begin{cases} b & \text{if } \mathbf{r}_{ij} = 0, \\ |\mathbf{r}_{ij}|^{-\alpha} & \text{otherwise} \end{cases} \quad (2)$$

and periodic boundary conditions (PBC). The distance between sites \mathbf{r}_{ij} is then given by the nearest image convention. Through this work we will focus on the case of attractive or ferromagnetic interaction, so the interaction strength is $\Gamma > 0$, although the extension to antiferromagnetic or repulsive models will be discussed. b is a parameter that can be tuned to shift the spectrum of J . The decay rate α sets the range of the interactions. For $\alpha < d$, where d is the dimensionality of the lattice, the interactions decay slowly enough that the sum in the coupling term (1) depends superlinearly on N , breaking the extensivity of the model (see Appendix A 1). Kac's renormalization factor $1/\tilde{N}$ restores extensivity, ensuring a well-defined thermodynamic limit. Here $\tilde{N} = \sum_i \tilde{J}_{ij}$, note that PBC make the model translation invariant, and thus $\sum_i \tilde{J}_{ij}$ is independent of j . Regardless, the model remains nonadditive in this regime. Nonadditivity brings about particular statistical and dynamical phenomena that differ from the commonly studied short-range models, such as ensemble inequivalence, negative specific heat, and quasistationary states [8]. Accordingly, the regime $\alpha < d$ is identified as (*strong*) *long range*. In the regime $\alpha > d$, the model is naturally extensive, and Kac's

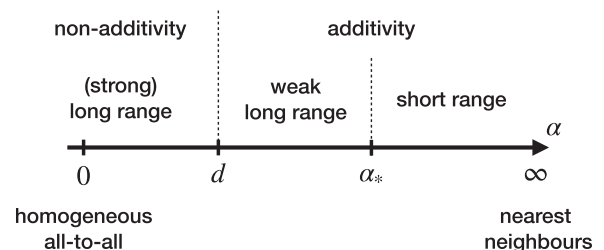


FIG. 1. Classification of long-range models following [5,8] valid for both the classical and quantum models. This work presents a solution for the quantum strong long-range regime.

renormalization factor amounts to a rescaling of the interaction strength. Within the regime $\alpha > d$ two further subregimes can be identified: for $\alpha > \alpha_*$ the critical exponents of the model match those of the nearest-neighbor model ($\alpha \rightarrow \infty$), this is the *short-range regime*; for $d < \alpha < \alpha_*$ the model presents critical exponents that differ from the short-range ones, the effects of long-range interactions are felt but the model is additive, this is the *weak long-range regime* [5,8]. For convenience, we summarize this classification in Fig. 1. *This work deals with the strong long-range regime.*

Strong long-range models are commonly disregarded in many analytical and numerical studies on the grounds of the ill-defined thermodynamic limit brought about by the nonextensivity. Kac’s rescaling eliminates this barrier, making their study possible. For quantum models, seminal numerical studies solving the transverse-field Ising model in the strong long-range regime are found in Refs. [20,21]. They confirm that in this regime the model is within the mean-field universality class. This is in agreement with the claim that mean field is exact for quantum spin models in the strong long-range regime [22] that generalizes similar findings in classical systems [23–26]. These works are crucial for the rigorous understanding of the physics of long-range systems. On the one hand, they provide an exact way to solve them; on the other hand, they provide a starting point for approximations that tackle the weak long-range regime.

This work provides a recipe to analytically solve, in the canonical ensemble, quantum strong long-range models. Therefore, it complements the work of Mori [22] and confirms that *in the strong long-range regime mean field is exact*. Besides, it extends the work of Campa and coworkers for classical strong long-range models to the quantum case [27]. Our work introduces a generalized Hubbard-Stratonovich transformation (HST) and provides a closed expression for the free energy at any temperature. Technically, we show how to use the equivalence between generalized Dicke models and interacting quantum models as a quantum HST. We show that only *strong* long-range models admit this mapping and formulate their canonical solution in terms of the associated Dicke model, which is then tackled following the prescription of Wang and Hioe [28,29]. We illustrate the method on the Ising chain in transverse field. We find that the critical behavior is universal for $\alpha < d$ and any lattice dimensionality. The expression for the magnetization (the order parameter) is shown to be equivalent to the mean-field solution, thus proving the exactness of the latter. Finally, we study the algebraic decay of correlations as a function of the decay rate of interactions α .

The rest of the paper is organized as follows. In Sec. II, we provide a brief overview of the HST as a tool to solve classical models, which forms the basis for our further development. In Sec. III, we establish the relationship between generalized Dicke and long-range models and introduce the generalized HST. Section IV presents the solution for strong long-range models and a discussion of which models can be treated with this method. We perform the calculations for the long-range transverse field Ising model, including the full phase diagram and the decay of two-point correlations in Sec. V. Finally, we conclude the paper with some general remarks and relegate more technical details to the Appendixes.

II. SKETCH OF THE SOLUTION FOR CLASSICAL SYSTEMS

To warm up, it is convenient to understand how to solve classical strong long-range models, mainly following the works of Campa and coworkers [23,27]. For simplicity consider the Ising model

$$\mathcal{H}_{cl} = h \sum_i s_i - \sum_{ij} J_{ij} s_i s_j. \quad (3)$$

Here, s_i is a discrete variable. The solution is based on two main observations. First, diagonalizing the interaction matrix $J = \Lambda D \Lambda^T$, which allows one to write the coupling term as $\sum_k D_k (\sum_i \Lambda_{ik} s_i)^2$, where $\{D_k\}$ are the eigenvalues of the interaction matrix. Note that, in this form, the coupling is written as a sum of interaction terms that are quadratic in $\sum_i \Lambda_{ik} s_i$. Second, eliminating these quadratic interactions by use of the Hubbard-Stratonovich transformation which is based on the equality

$$Z = \sum_{s_i} e^{-\beta \mathcal{H}_{cl}} \propto \int \prod_k du_k \sum_{s_i} e^{-\beta (h \sum_i s_i + \sum_k u_k^2 / D_k - 2 \sum_{ik} \Lambda_{ik} s_i u_k)}, \quad (4)$$

where u_k are real auxiliary variables. This equality for the partition function follows from Gaussian integral formulas.

Notice that we have decoupled the interaction $J_{ij} s_i s_j$, therefore, the sum over s_i configurations is trivial. Finally, the integral over the real variables u_k can be done within the saddle-point approximation in the N -large limit. This is true if some conditions are met on the eigenspectrum of the J_{ij} matrix (see below and the discussion in Appendix B).

III. FROM THE DICKE MODEL TO QUANTUM LONG-RANGE MODELS AND BACK

A. Effective theory of the Dicke model

The method described above and utilized in Ref. [27] cannot be straightforwardly applied to quantum models. The application of the HST requires splitting the exponential that constitutes the kernel of the partition function into a product of exponentials, which in the quantum case is prevented by the noncommutativity of the long-range interaction term and other terms in the Hamiltonian. There are ways in which the HST can be applied to solve quantum systems, but it requires a reframing of the partition function in terms of commuting quantities. A field-theory formulation or imaginary-time Trotterization are examples of this. Here we present an alternative which is the closest to the classical formulation.

Our method utilizes some results from quantum optics in order to draw an equivalence between some quantum long-range models and a cavity QED model. Specifically, we utilize the generalized Dicke model as our starting point to develop this equivalence:

$$\mathcal{H} = \sum_{k=0}^{M-1} \omega_k a_k^\dagger a_k + \mathcal{H}_0 - \sum_{k,i} (a_k + a_k^\dagger) \frac{\lambda_{ik}}{\sqrt{N}} C_i. \quad (5)$$

Here \mathcal{H}_0 is an exactly solvable Hamiltonian of the “matter” degrees of freedom and C_i is the local Hermitian operator

that couples site i to the bosonic modes with $[a_k, a_{k'}^\dagger] = \delta_{k,k'}$; finally, λ_{ik} are real coupling constants. In two previous publications [30,31] we show that the generalized Dicke model, after integrating out the electromagnetic modes, yields an exact effective Hamiltonian description for the matter degrees of freedom alone in the limit $N \rightarrow \infty$ (thermodynamic limit). The resulting Hamiltonian,

$$\mathcal{H}_m^{\text{eff}} = \mathcal{H}_0 - \sum_{ij} \sum_{k=0}^{M-1} \frac{\lambda_{ik} \lambda_{jk}}{N \omega_k} C_i C_j, \quad (6)$$

corresponds to a quantum model with interactions given by $(J_{\text{eff}})_{ij} = \sum_k^{M-1} \lambda_{ik} \lambda_{jk} / (N \omega_k)$. The mode structure of the cavity determines the resulting effective model. However, it is important to note that the exact mapping between Hamiltonians (5) and (6) is limited to the thermodynamic limit $N \rightarrow \infty$ and a number of modes M such that $\lim_{N \rightarrow \infty} M/N = 0$. Following, we demonstrate how we can reverse the effective theory to solve a quantum model. The first question that arises is which family of quantum models, with interaction given by Eq. (1), can be solved this way, i.e., which can be cast in the form of Eq. (6). We also show that this is the case for strong long-range models, $\alpha < d$; this is the first result of this paper.

B. Mapping a quantum model to the Dicke model

If we start from an arbitrary extensive¹ model of the form $\mathcal{H}_m = \mathcal{H}_0 - \sum_{ij} J_{ij} C_i C_j$ [cf. Eq. (1)], the first step is to diagonalize the interaction matrix $J = \Lambda D \Lambda^T$, where D is a diagonal matrix, $D_{kp} \equiv D_k \delta_{kp}$. Note that Λ is orthogonal because J is symmetric. The matrix elements are then given by

$$J_{ij} = \sum_{k=0}^{N-1} \Lambda_{ik} D_k \Lambda_{jk}. \quad (7)$$

Assuming that $J_{ij} > 0$, the smallest eigenvalue of J can always be set to zero by adjusting its diagonal elements, which we denote b . Fixing $b \neq 0$ introduces, generally, nontrivial diagonal terms of the form $\Gamma b / \tilde{N} C_i^2$. These can be shown to be negligible in the thermodynamic limit, so the freedom to set b remains (see Appendix A2). For a general interaction matrix the number of nonzero eigenvalues M scales with the size of the matrix N . Conveniently, it can be shown that for a model with power-law decaying interactions and PBC such as the one considered in this work (1), the number of nonzero modes in the thermodynamic limit ($N \rightarrow \infty$) depends on the decay rate of the interaction [27]. For a model in the strong long-range regime $\alpha < d$, only a small number of modes have a nonzero eigenvalue, such that $\lim_{N \rightarrow \infty} M/N = 0$. This can be seen analytically in models with a translation-invariant interaction matrix, which can be diagonalized in Fourier space, obtaining a closed expression for its eigenvalues:

$$D(\mathbf{q}) = \frac{\Gamma}{\tilde{N}} \sum_{\mathbf{r}} \tilde{J}(\mathbf{r}) \exp[-i\mathbf{q}\mathbf{r}]. \quad (8)$$

¹Meaning that Kac's prescription is used to ensure extensivity if the model is strong long ranged.

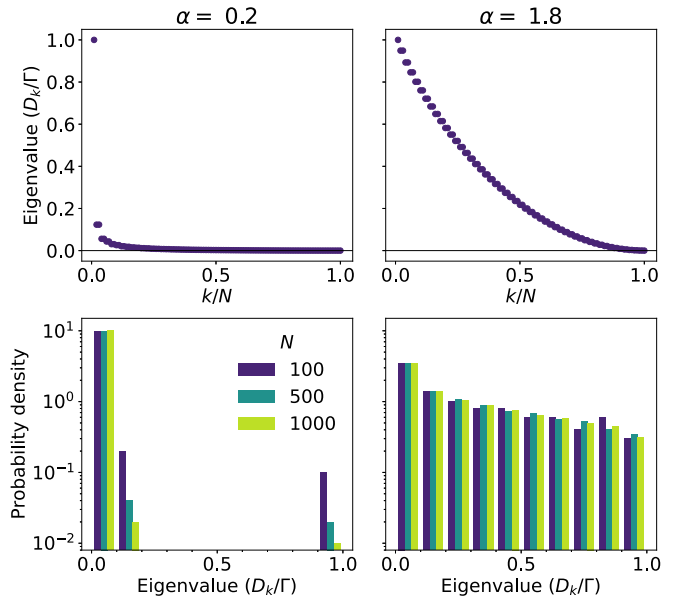


FIG. 2. Analysis of the eigenvalues of the coupling matrix J (1) for $d = 1$. Left: For $\alpha = 0.2 < 1$, a plot of the eigenvalues for $N = 100$ on top and a histogram of the eigenvalues as a function of N on the bottom. Right: Same but for $\alpha = 1.8 > 1$.

Here \mathbf{q} denotes any of the N reciprocal-space vectors in the first Brillouin zone and the sum runs over all lattice points. The large- N behavior of $D(\mathbf{q})$ can then be estimated by replacing the sum with an integral [27].

Complementarily, we provide in Fig. 2 a graphical analysis of this phenomenon by showing the typical distribution of eigenvalues depending on α for $d = 1$ (the same behavior is observed in other dimensions, not shown). This graphical analysis can be useful for models without translation invariance. In Fig. 2 we show that for a strong long-range model the eigenvalues bunch around zero as N increases, whereas they remain more uniformly distributed in the weak long-range regime. This can be condensed into a criterion for determining whether arbitrary models are tractable: knowing that the eigenvalues of J are non-negative and bounded by construction, if only a vanishingly small fraction M/N are nonzero for $N \rightarrow \infty$, then their average will tend to zero and vice versa. Thus, for an arbitrary interaction matrix J , if

$$\lim_{N \rightarrow \infty} \frac{1}{N} \sum_{k=0}^{M-1} D_k = \lim_{N \rightarrow \infty} \frac{1}{N} \text{Tr}(J) = 0 \quad (9)$$

the model is tractable, i.e., the number M of nonzero eigenvalues scales as $\lim_{N \rightarrow \infty} M/N = 0$. If we apply this criterion to translation-invariant models we find $\lim_{N \rightarrow \infty} 1/N \sum_k D_k = \lim_{N \rightarrow \infty} \Gamma b / \tilde{N}$, which is zero for $\alpha < 1$ and nonzero otherwise (see Appendixes A1 and A2).

Once it is established that a given model has a sufficiently small number of nonzero eigenvalues, one can sort them by decreasing value and truncate the sum in Eq. (7) to consider only the first M terms for which $D_k \neq 0$. For these remaining nonzero eigenvalues, we can identify $\omega_k = 1/D_k$. This, together with the rescaled elements of the change of basis

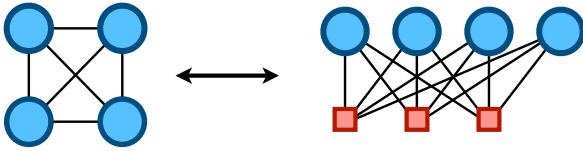


FIG. 3. Schematic of the generalized Hubbard-Stratonovich transformation mapping a quantum long-range model to (and from) a generalized Dicke model. Blue dots represent “matter” degrees of freedom and red squares represent cavity modes [cf. Hamiltonians (5) and (6) in the main text].

matrix $\lambda_{ik} = \sqrt{N}\Lambda_{ik}$, leads to Eq. (6) and effectively defines the mode structure for the associated Dicke model (5).

In summary, models for which $\lim_{N \rightarrow \infty} M/N = 0$, in particular strong long-range models, can be mapped to generalized Dicke models via the effective theory described in [30,31]. To gain further insight, it is useful to compare Hamiltonians (5) and (6) with the system depicted in Fig. 3, which outlines our procedure. The interacting model, shown in the left-hand side of the figure, where constituents are depicted as blue nodes and interactions as black edges, is mapped to a larger system where the *physical* (matter) degrees of freedom are uncoupled and interact with *auxiliary* bosonic modes represented as red squares.² Integrating out these bosonic modes would lead back to the desired interactions J_{ij} . The parallelism between the auxiliary bosonic modes in the effective theory and the auxiliary classical fields in the standard HST motivates *the claim of a generalized Hubbard-Stratonovich transformation*.

IV. EXACT SOLUTION OF STRONG LONG-RANGE MODELS

At this point we have shown how to map a strong long-range quantum model (1) to a generalized Dicke model (5) as illustrated in Fig. 3. To solve the latter, we will follow the steps outlined in the original solution of the Dicke model by Wang and Hioe [28,29]. In the thermodynamic limit, the trace over the photonic degrees of freedom is replaced by a collection of complex Gaussian integrals and the bosonic creation and annihilation operators a_k^\dagger, a_k , are replaced by complex fields α_k^*, α_k :

$$Z = \int \prod_{k=0}^{M-1} \frac{d^2\alpha_k}{\pi} \text{Tr}_m \left\{ \exp \left[-\beta \left(\sum_{k=0}^{M-1} \omega_k |\alpha_k|^2 + \mathcal{H}_0 + \sum_{k,i} \frac{2\lambda_{ik}x_k}{\sqrt{N}} C_i \right) \right] \right\}, \quad (10)$$

where $\alpha_k = x_k + iy_k$. At this point, the parallelism with the standard Hubbard-Stratonovich transformation used in

²Figure 3 is actually an oversimplification, as it only depicts long-range interactions, which are the ones replaced by the auxiliary bosonic modes of the effective theory. The theory is also applicable to models containing a combination of short- and long-range interactions. For a discussion about the applicability of the method, see Sec. IV.

the classical model is even more explicit. The Gaussian integral over the imaginary parts $\{y_k\}$ yields an unimportant constant. To tackle the integration over the real parts, we perform a change of variables $u_k^2 = x_k^2/N$ and define

$$Z_m[u_k] \equiv Z_m(u_0, \dots, u_{M-1}) = \text{Tr}_m \{ e^{-\beta(\mathcal{H}_0 + \sum_{k,i} 2\lambda_{ik}u_k C_i)} \} \quad (11)$$

and $f_m[u_k] = \ln(Z_m[u_k])/N$. In the resulting integral

$$Z = \int \prod_{k=0}^{M-1} \sqrt{\frac{N}{\pi\omega_k}} du_k \exp(N\phi[u_k]), \quad (12)$$

where

$$\phi[u_k] = -\beta \sum_{k=0}^{M-1} \omega_k u_k^2 + f_m[u_k], \quad (13)$$

the exponent depends explicitly linearly on N , allowing one to use the saddle-point method (exactly for $N \rightarrow \infty$) to express the partition function as the value of the integrand at the maximum of $\phi[u_k]$:

$$Z = \prod_{k=0}^{M-1} \sqrt{\frac{N}{\pi\omega_k}} \exp(N\phi[\bar{u}_k]), \quad (14)$$

with

$$\phi[\bar{u}_k] = \max_{\{u_k\}} \phi[u_k]. \quad (15)$$

Computing the partition function is thus reduced to a multivariate maximization problem. In order for the zero-order saddle-point approximation to be exact, one has to verify that there exists a maximum $\{\bar{u}_k\}$, i.e., that ϕ admits a stationary point $\{\bar{u}_k\}$ and the eigenvalues of the Hessian of ϕ at the stationary point $H_\phi[\bar{u}_k]$ are all negative. In the presence of several maxima, one has to find the global maximum. Finding global extrema of a multivariate scalar function is normally a complex task, without guarantee or provability of success, but in the present case it is greatly facilitated for homogeneous or near-homogeneous systems (see Sec. V). Additionally, the second-order corrections to the partition function in the form of a factor $(\det H_\phi[\bar{u}_k])^{-1/2}$ must be negligible with respect to the zero-order term $\exp\{N\phi[\bar{u}_k]\}$, but this is generally true (see Appendix B). *This is the main result of this paper, i.e., the exact expression for the partition function of strong long-range models (14).*

In the next section and in order to give concrete formulas, we particularize for the case of the Ising model in transverse field. However, the ideas presented here can be applied to other models. For instance, our next section generalizes easily to a spin- s system where $s > \frac{1}{2}$ and also to the inclusion of a longitudinal field, such that $\mathcal{H}_0 = \omega_z \sum_i S_i^z + \omega_x \sum_i S_i^x$ and $C_i = 2S_i^x$ with $[S_i^\alpha, S_j^\beta] = i\epsilon_{\alpha\beta\gamma} S_i^\gamma \delta_{ij}$ spin- s operators. The Fermi-Hubbard model with long-range interactions could also be treated with our method. Here $\mathcal{H}_0 = t_{ij} c_i^\dagger c_j$ and $C_i = c_i^\dagger c_i$ with $\{c_i, c_j^\dagger\} = \delta_{ij}$ fermionic operators. Finally, we could consider for \mathcal{H}_0 any model such that $\mathcal{H}_0 + \sum_i \xi_i C_i$ is solvable, where the ξ_i are constants. In doing so, we could combine short-range models (as the one-dimensional short-range Ising

model in transverse field, the XY model, and so on) with strong long-range interactions. This is because our method requires knowledge of the eigenstates of $\mathcal{H}_0 + \sum_{k,i} 2\lambda_{ik}u_k\mathcal{C}_i$ [cf. Eq. (11)].

We have, thus far in the paper, focused only on ferromagnetic (attractive) models. However, the discussion of the applicability and generalizations of our method demands that we consider antiferromagnetic (repulsive) models [32,33]. Frustrated antiferromagnetic long-range models cannot be tackled with our method. To see why, it suffices to look at Fig. 2, frustrated antiferromagnetic models arise from changing the global sign of the interaction in Eq. (1), which in turn results in a change of sign of the eigenvalues of the coupling matrix. For a general model, a shift to render the smallest eigenvalue equal to zero is not possible as it would require a b of the order of \tilde{N} , leading to nonvanishing diagonal elements even in the $N \rightarrow \infty$ limit. For a model in which $\mathcal{C}_i^2 = 1$, the shift is possible, but after a shift to render the smallest eigenvalue equal to zero, we find that the majority of the eigenvalues are nonzero, regardless of the range of interactions α . In contrast, it is possible to define unfrustrated long-range antiferromagnetic models $J_{ij} = \Gamma(-1)^{i+j}J(\mathbf{r}_{ij})/\tilde{N}$, as an extension of unfrustrated nearest-neighbor antiferromagnetic interactions [34]. Here, the sign change is alternating, rather than global, effectively defining two sublattices. The interaction matrix defined this way shares the eigenvalues of its ferromagnetic counterpart and the corresponding model can thus be tackled with our method. However, a number of interesting subtleties arise later on in the solution that deserve a detailed discussion; we reserve this for a future publication.

V. SOLUTION OF THE LONG-RANGE ISING MODEL IN A TRANSVERSE FIELD

To showcase the effectiveness of the formalism presented in the previous sections, we particularize now to an Ising chain in transverse field

$$\mathcal{H} = \frac{\omega_z}{2} \sum_i \sigma_i^z - \sum_{ij} J_{ij} \sigma_i^x \sigma_j^x, \quad (16)$$

where $\sigma^{x,z}$ are the usual Pauli matrices and J_{ij} is given by Eq. (2). This corresponds to setting $d = 1$, $\mathcal{H}_0 = \frac{\omega_z}{2} \sum_i \sigma_i^z$, and $\mathcal{C}_i = \sigma_i^x$. In Appendix C 1 we show that this leads to

$$\phi[u_k] = -\beta \sum_{k=0}^{M-1} \omega_k u_k^2 + \frac{1}{N} \sum_i \ln[2 \cosh(\beta \epsilon_i)], \quad (17)$$

with $2\epsilon_i[u_k] = \sqrt{\omega_z^2 + 4(2 \sum_k \lambda_{ik} u_k)^2}$.

In the case of a homogeneous \mathcal{H}_0 we show in Appendixes C 2 and C 3 that the global maximum is homogeneous in the lattice. In terms of the minimization variables, homogeneity implies that $u_0 = u \neq 0$ and $u_{k \neq 0} = 0$ (see Appendix C 2). This means that only the zero mode, which is constant on the lattice, $\lambda_{i0} = 1 \forall i$, is relevant in determining the thermodynamic properties of the model. In turn, one finds that the critical properties of the model are independent of the decay rate of interactions α since the latter only determines the degree to which higher-frequency modes ($k > 0$) have to

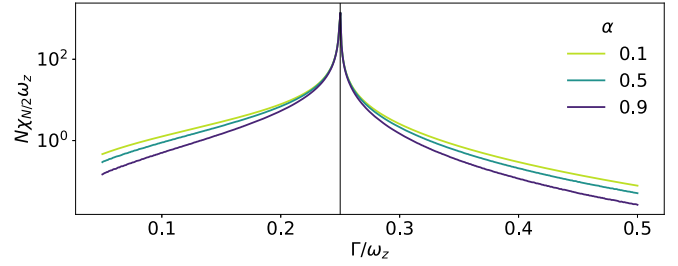


FIG. 4. Susceptibility for maximally separated spins $\chi_{N/2}$ for strong long-range quantum Ising models as a function of the interaction strength Γ . The parameters used were $\omega_z = 1$, $\beta\omega_z = 10$ and $N = 100$.

be considered in the diagonalization of J . In more intuitive terms, homogeneity is revealed in the fact that $2\epsilon_i = 2\epsilon = \sqrt{\omega_z^2 + 16u^2}$, $\forall i$. In any case, the multivariate maximization problem simplifies to a single variable maximization problem $\max_u \phi(u)$. Taking the derivative of ϕ with respect to u yields the condition

$$\bar{u}\bar{\epsilon} = 2\Gamma\bar{u} \tanh(\beta\bar{\epsilon}), \quad (18)$$

which is manifestly α independent. Note that $\bar{\epsilon} = \epsilon(\bar{u})$. For $\Gamma < \omega_z/4$, $\bar{u} = 0$ is the only solution. For $\Gamma > \omega_z/4$, the solution depends on β , for $\beta > \beta_c$, with β_c given by $\omega_z = 4\Gamma \tanh(\beta_c \omega_z/2)$, there is another solution to Eq. (18) given by $\bar{\epsilon} = 2\Gamma \tanh(\beta\bar{\epsilon})$. The solution $\bar{u} = 0$ corresponds to a maximum in the regime where it is the only solution and becomes a minimum for $\beta > \beta_c$ with the maximum given by the other solution [28]. This marks the paramagnetic-ferromagnetic transition point. This is the well-known mean-field critical behavior of the standard (single-mode homogeneous coupling) Dicke model [28,35], which is shared by the Lipkin-Meshkov-Glick (LMG) model (all-to-all homogeneous Ising) [36,37] and, as we just showed, is also universal to all strong long-range Ising models and their associated Dicke models, i.e., we have demonstrated that the critical point is independent of α . This can be visualized in Fig. 4 where the vertical line marks the phase transition, located at the maximum for the susceptibility (see below), and is independent of α . Besides, in Fig. 5 we compute the critical line, in red, in the $(\Gamma, 1/\beta)$ plane and compare it against the simulations in Ref. [21]. We find excellent agreement with their numerical results and showcase that the critical point is independent of α and coincides with the mean-field value.

In terms of observables, we focus now on the calculation of magnetization. In order to do so from the partition function, we introduce a perturbative longitudinal field to the Hamiltonian, such that $\mathcal{H} \rightarrow \mathcal{H} - \sum_i h_i \sigma_i^x$. Then one can compute the order parameter $\beta\langle\sigma_i^x\rangle = \partial \ln Z / \partial h_i$ and the susceptibilities³

$$\chi_{ij} = \lim_{\{h_n\} \rightarrow 0} \frac{\partial \langle \sigma_i^x \rangle}{\partial h_j}. \quad (19)$$

³The magnetization must be kept $\{h_n\}$ dependent in order to compute the susceptibility; the magnetization of the $\{h_n\}$ -independent model is defined as $\beta\langle\sigma_i^x\rangle = \lim_{\{h_n\} \rightarrow 0} \partial \ln Z / \partial h_i$.

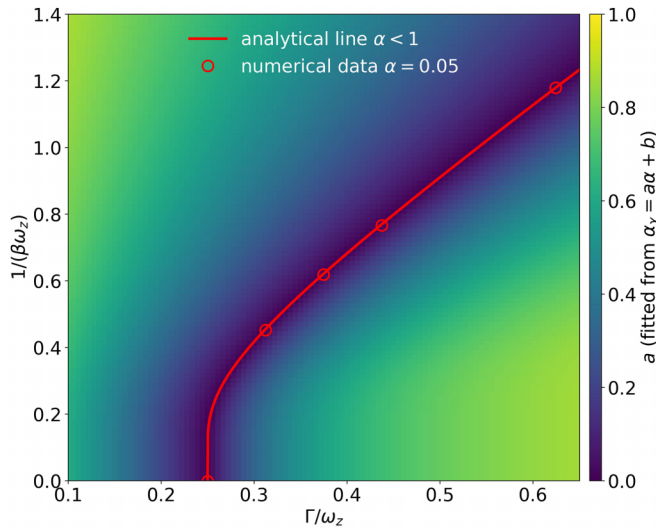


FIG. 5. Phase diagram of the strong long-range Ising chain in transverse field. The red line corresponds to the universal critical line for $\alpha < 1$. The numerical data are taken from Ref. [21]. The color map shows the slope of the linear dependence $\alpha_\chi = a\alpha + b$, where α_χ is susceptibility decay rate and α is the rate of decay of interactions, computed with parameters $\omega_z = 1$ and $N = 100$.

The introduction of longitudinal fields leads to the substitution $2 \sum_k \lambda_{ik} u_k \rightarrow 2 \sum_k \lambda_{ik} u_k + h_i$ in Eq. (17). The magnetization is then

$$\langle \sigma_i^x \rangle = \tanh(\beta \epsilon_i [\bar{u}_k]) \frac{2 \sum_{k=0}^{M-1} \lambda_{ik} \bar{u}_k + h_i}{\epsilon_i [\bar{u}_k]}. \quad (20)$$

Here, the magnetization appears as a function of the maximization variables $\{\bar{u}_k\}$. However, it is possible to show that $\sum_k \lambda_{ik} \bar{u}_k = \sum_j J_{ij} \langle \sigma_j^x \rangle$, rewriting Eq. (20) as a self-consistent equation on $\{\langle \sigma_i^x \rangle\}$ which is precisely the self-consistent equation that arises in a mean-field solution. Our exact analytical method is thus equivalent to mean-field theory, proving that mean-field theory is exact for strong long-range models and any lattice dimensionality d . Anecdotally, our theory evidences that the self-consistent solution from mean-field theory is redundant, in the sense that the solution involves a transcendental equation of N variables (the magnetizations $\{\langle \sigma_i^x \rangle\}$), whereas the same problem can be rewritten in terms of M variables (the $\{u_k\}$), with $\lim_{N \rightarrow \infty} M/N = 0$.

A. Decay of correlations

Our final result concerns the decay of correlations. In weak long-range and short-range systems correlations decay exponentially at long distances. Only at the critical point do these systems exhibit power-law decay of correlations [14–16]. Conversely, strong long-range systems exhibit power-law decay of correlations at all distances. In the absence of exponential decay, the concept of correlation length cannot be straightforwardly defined, although there have been some attempts [38]. Here we study the susceptibility χ_{ij} [Eq. (19)] as a measure of correlations between spins, as it is proportional to the Kubo

correlator [39][Chap. 4]

$$\chi_{ij} = \beta \left(\frac{1}{Z} \int_0^\beta \text{Tr}(e^{-(\beta-s)\mathcal{H}} \sigma_i^x e^{-s\mathcal{H}} \sigma_j^x) - \langle \sigma_i^x \rangle \langle \sigma_j^x \rangle \right). \quad (21)$$

The susceptibility can be computed analytically from Eq. (19) for a translation-invariant model [40][Chap. 6] (see Appendix D for a derivation) or numerically otherwise. The analytical derivation yields

$$\chi_{ij} = Y \delta_{ij} + \frac{1}{N} \sum_{k=0}^{M-1} \lambda_{ij} (\chi_k - Y) \lambda_{jk}, \quad (22)$$

where Y is a quantity that depends on \bar{u} [Eq. (D4)] and $\{\chi_k\}$ are the Fourier modes of the susceptibility [Eq. (D7)]. Equation (22) evidences that $\chi_{i \neq j}$ goes to zero in the thermodynamic limit with a speed that is determined by the ratio M/N and thus ultimately by α (by its relation to d).

For a numerical calculation, the introduction of a site-dependent field h_i breaks the homogeneity of the model and the multivariate maximization of ϕ is carried out numerically; $\langle \sigma_i^x \rangle$ is then computed according to Eq. (20) and χ_{ij} is computed as a finite difference. We have verified that both methods yield the same results for the current model. This is noteworthy because the numerical calculation relies on a multivariate optimization which could, *a priori*, converge to an incorrect result corresponding to a local maxima. We believe the success is due to the fact that the only deviation from homogeneity stems from the introduction of a perturbative field and is thus small. Hence, although the optimization is strictly multivariate, the landscape does not differ much from the univariate case.

Despite the fact that the analytical results have been obtained under the assumption that we worked in the thermodynamic limit $N \rightarrow \infty$. The computation of the susceptibility, whether numerically or according to Eq. (22), requires us to fix a finite value of N and M . For each value of α and N , we increase the value of M until convergence is reached while enforcing the constraint that $\lim_{N \rightarrow \infty} M(N)/N = 0$.

Because the model is translation invariant, the susceptibility is only a function of distance, allowing us to define $\chi_{ii+r} \equiv \chi_r$. In Fig. 4 we study the susceptibility at a fixed distance: we plot the half-chain susceptibility $\chi_{N/2}$ as a function of the interaction strength Γ for different decay rates $\alpha < 1$ at zero temperature $\beta \rightarrow \infty$. The half-chain susceptibility displays α -independent divergence at the critical point and some dependence on α away from it. Intuitively, the correlations remain larger for longer-ranged models. We now turn to the spatial dependence of the susceptibility. In the absence of a correlation length, we study the susceptibility decay rate α_χ , defined from the relation $\chi_r = Ar^{-\alpha_\chi}$. Interestingly, one finds that α_χ depends linearly on α , $\alpha_\chi = a\alpha + b$. In Fig. 5 we plot the slope a as a function of interaction strength Γ and inverse temperature $1/\beta$. Close to the critical line, the susceptibility decay rate α_χ becomes independent of the interaction decay rate α , in agreement with Fig. 4. As one moves further from the critical line, $a \rightarrow 1$, varying continuously from 0 to 1 in intermediate regions. In all cases we find $b \approx 0$. Similar algebraic decays have been described previously for the connected correlator $\langle \sigma_1^x \sigma_r^x \rangle - \langle \sigma_1^x \rangle \langle \sigma_r^x \rangle$ in the paramagnetic phase [14].

There, a linear relation between α_χ and α is also reported. Here we extend those findings to the full phase diagram.

VI. CONCLUSIONS

In this paper, we have presented a method for solving strong long-range models in the quantum domain based on the Hubbard-Stratonovich transformation for classical systems. Our method is a physics-based solution rooted in light-matter interaction models in which, in the thermodynamic limit, light can be integrated out leaving an effective long-range model. Solutions of the former, i.e., Dicke models, are due to Hepp and Lieb [41,42], and Wang and Hioe [28,29], which we have recently generalized [30,31].

We have shown that our method can be applied in the strong long-range regime and confirmed that mean-field theory is exact in this regime [cf. Fig. 1 and Eqs. (2), (5), and (6)]. In doing so, this paper complements the work of Mori [22]. Besides, it extends the work of Campa and coworkers for classical strong long-range models to the quantum case [27]. It is worth noting that neither our method nor the equivalent mean-field theory can be used to compute nonlocal quantities such as the entanglement entropy, which can be nontrivial in strong long-range systems [43].

Our method is flexible and could be applied, e.g., to spin- s systems where $s > \frac{1}{2}$, to models with a longitudinal field, such as the long-range XXZ model, or to the Fermi-Hubbard model with long-range interactions. Additionally, many exactly solvable models could be complemented with long-range interactions and solved with our method since it relies on knowing the eigenvalues of the system without long-range interactions and with a “field” term proportional to the long-range coupling operator. Unfrustrated antiferromagnetic systems are also within the scope of the method. In conclusion, our work provides a powerful tool for solving quantum long-range models.

ACKNOWLEDGMENTS

We thank A. Campa and T. Mori for discussing and explaining details of their previous results; they were of great help in completing this work. The authors acknowledge funding from the EU (QUANTERA SUMO and FET-OPEN Grant No. 862893 FATMOLS), the Spanish Government Grants No. PID2020-115221GB-C41/AEI/10.13039/501100011033 and No. TED2021-131447B-C21 funded by MCIN/AEI/10.13039/501100011033 and the EU “NextGenerationEU”/PRTR, the Gobierno de Aragón (Grant No. E09-17R Q-MAD) and the CSIC Quantum Technologies Platform PTI-001. This work has been financially supported by the Ministry of Economic Affairs and Digital Transformation of the Spanish Government through the QUANTUM ENIA project call Quantum Spain project, and by the European Union through the Recovery, Transformation and Resilience Plan NextGenerationEU within the framework of the “Digital Spain 2026 Agenda.” J.R.-R. acknowledges support from the Ministry of Universities of the Spanish Government through the Grant No. FPU2020-07231.

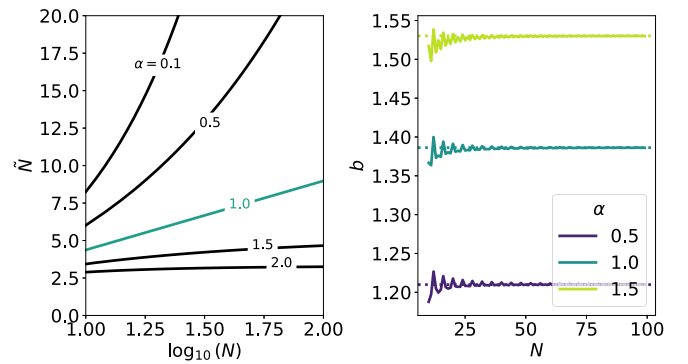


FIG. 6. Scaling of $\tilde{N} = \sum_j \tilde{J}_{ij}$ (left) and b (right) for a one-dimensional model ($d = 1$) with power-law decaying interactions (1). Here b is fixed such that the smallest eigenvalue of \tilde{J} is zero. The dotted lines indicate the analytical asymptote.

APPENDIX A: PROPERTIES OF THE LONG-RANGE INTERACTION MATRIX

1. Loss of extensivity

In Fig. 6 we illustrate the extensivity (or lack thereof) of a model with power-law decaying interactions in $d = 1$. We compute $\tilde{N} = \sum_j \tilde{J}_{ij}$ as a measure of the coupling energy per spin. In the absence of Kac’s rescaling, this quantity must not scale with the number of spins N to keep the total coupling energy extensive. Figure 6 shows that this is not the case for $\alpha < 1$. The threshold case $\alpha = 1$ is highlighted for clarity and corresponds to a logarithmic dependence of \tilde{N} on N . For $\alpha > 1$ the dependence is sublogarithmic, i.e., \tilde{N} becomes independent of N at large N . As discussed in the main text, loss of extensivity is prevented with Kac’s rescaling, which we can now understand as a renormalization of the total coupling energy by the energy per spin.

In fact, for $d = 1$ and $N \rightarrow \infty$ the scaling of \tilde{N} can be computed analytically since

$$\tilde{N} = \sum_i^N \tilde{J}_{ij} = b + 2 \sum_{r=1}^{\infty} r^{-\alpha}. \quad (\text{A1})$$

As b converges to a constant value when $N \rightarrow \infty$ (will be shown in Appendix A 2), the convergence of \tilde{N} will be ruled by the convergence of the infinite series. For $\alpha > 1$ the series is convergent, so \tilde{N} becomes independent of N at large N . For $\alpha \leq 1$ the series diverges.

2. Diagonal terms can be neglected in strong long-range models

Setting $b \neq 0$ introduces a new diagonal term in the Hamiltonian

$$- \sum_i^N \Gamma b / \tilde{N} C_i^2. \quad (\text{A2})$$

Importantly, this term contains a factor b/\tilde{N} . We know from Appendix A 1 that $\lim_{N \rightarrow \infty} \tilde{N} = \infty$ for $\alpha < d$. So if b is independent of N for $N \rightarrow \infty$, the diagonal term vanishes in the thermodynamic limit.

It can be shown analytically that this is the case for $d = 1$ and $\alpha > 0$. From Eq. (8) we see that the smallest eigenvalue

of J when $N \rightarrow \infty$ is given by

$$D_{\min} = \frac{\Gamma}{\bar{N}} \sum_{\mathbf{r}} \tilde{J}(\mathbf{r})(-1)^r = \frac{\Gamma}{\bar{N}} \left(b + 2 \sum_{r=1}^{\infty} (-1)^r r^{-\alpha} \right). \quad (\text{A3})$$

Here $r = |\mathbf{r}|$. Hence, setting $D_{\min} = 0$ fixes

$$b = -2 \sum_{r=1}^{\infty} (-1)^r r^{-\alpha}. \quad (\text{A4})$$

The convergence of this series is proven by means of the alternating series test since the absolute value of its terms monotonically decrease to 0. For $\alpha = 0$ and finite N , as $\tilde{J}_{i \neq j} = 1$, b must be fixed to 1 to ensure that the smallest eigenvalue of \tilde{J} is zero. This is manifestly independent of N .

In other dimensions or other models, this test can be done graphically. In Fig. 6 we show the value of b , for a model with power-law decaying interactions in $d = 1$, computed numerically for different values of N when b is chosen so that the smallest eigenvalue of J is zero. One can see that in this case the numerical results converge to the analytical prediction. The same behavior is observed in other dimensions.

APPENDIX B: NEGLIGIBLE SECOND-ORDER CORRECTIONS TO THE SADDLE-POINT METHOD

The second-order term of the saddle-point expansion is proportional to $(\det H_{\phi}[\bar{u}_k])^{-1/2}$. Accordingly, it corresponds to a correction to the free energy per particle of the form

$$\frac{1}{N} \ln(\det H_{\phi}[\bar{u}_k]) = \frac{1}{N} \sum_{k=0}^{M-1} \ln v_k \propto \frac{M}{N}, \quad (\text{B1})$$

where the $\{v_k\}$ are the eigenvalues of $\det H_{\phi}[\bar{u}_k]$. This correction scales as M/N and thus vanishes in the thermodynamic limit. Notably, if the applicability of the effective theory to map a long-range interacting model to a generalized Dicke model constitutes the first appearance of the restriction $\lim_{N \rightarrow \infty} M/N = 0$, the argument contained in this Appendix constitutes a second independent one. In fact, this second occurrence of the restriction also appears in classical systems, where it is actually the only restriction to $\lim_{N \rightarrow \infty} M/N = 0$, as in classical systems an unrestricted standard HST can be used, as outlined in Sec. II.

APPENDIX C: SOLVING THE LONG-RANGE ISING MODEL IN TRANSVERSE FIELD

1. Solving the associated Dicke model

Particularizing Eq. (11) for the Ising model, we have to compute

$$Z_m[u_k] = \text{Tr}_m \left\{ \exp \left[-\beta \sum_i^N \left(\frac{\omega_z}{2} \sigma_i^z + \sum_{k=0}^{M-1} 2\lambda_{ik} u_k \sigma_i^x \right) \right] \right\}. \quad (\text{C1})$$

Because the spins are now decoupled, the trace over spins factorizes. The resulting single-spin Hamiltonian has eigenvalues

$$\epsilon_i^{\pm} = \pm \epsilon_i = \pm \frac{1}{2} \sqrt{\omega_z^2 + 4 \left(\sum_{k=0}^{M-1} 2\lambda_{ik} u_k \right)^2}. \quad (\text{C2})$$

Accordingly,

$$Z_m[u_k] = \prod_i 2 \cosh(\beta \epsilon_i), \quad (\text{C3})$$

$$f_m[u_k] = \frac{1}{N} \sum_i \ln(2 \cosh \beta \epsilon_i), \quad (\text{C4})$$

$$\phi_m[u_k] = -\beta \sum_k \omega_k u_k^2 + \frac{1}{N} \sum_i \ln(2 \cosh \beta \epsilon_i). \quad (\text{C5})$$

2. Existence of a homogeneous maximum of ϕ

To find the maximum of $\phi[u_k]$ we impose a vanishing gradient $\nabla \phi = 0$, which translates to the following condition for the maximization variables:

$$\bar{u}_k \omega_k = \frac{1}{N} \sum_i^N \tanh(\beta \bar{\epsilon}_i) \frac{\lambda_{ik} 2 \sum_{l=0}^{M-1} \lambda_{il} \bar{u}_l}{\bar{\epsilon}_i}. \quad (\text{C6})$$

From here, let us consider a solution that is homogeneous in the lattice, we will later prove that possible inhomogeneous maxima are only local maxima in Appendix C3. Let us define $\mu_i = 2 \sum_k \lambda_{ik} u_k$ and consider it as an alternate optimization variable. Homogeneity implies that $\bar{\mu}_i \equiv \bar{\mu}$; to see how this affects the variables $\{\bar{u}_k\}$ it is useful to invert the relation and write u_k in terms of the $\{\mu_i\}$, yielding

$$u_k = \frac{1}{2N} \sum_i^N \lambda_{ik} \mu_i. \quad (\text{C7})$$

Now, homogeneity implies

$$\bar{u}_k = \frac{\bar{\mu}}{2N} \sum_i^N \lambda_{ik}. \quad (\text{C8})$$

Since the $\{\lambda_{ik}\}$ are the Fourier modes resulting from the diagonalization of J , we have $\sum_i \lambda_{ik} = N \delta_{k0}$. Accordingly, we find $\bar{u}_{k \neq 0} = 0$ and $2\bar{u}_0 = \bar{\mu}$. So, if the solution is homogeneous, the only relevant mode is the zero mode $\bar{u}_0 \equiv \bar{u}$ and the rest of the maximization variables are zero, with \bar{u} satisfying the condition

$$\bar{u} \omega_0 = \frac{2\bar{\mu}}{\bar{\epsilon}} \tanh(\beta \bar{\epsilon}). \quad (\text{C9})$$

From Eq. 8 we have $\omega_0 = 1/\Gamma$, which when replaced in Eq. (C9) yields Eq. (18).

At this point we can compute the Hessian of ϕ , H_{ϕ} . As we have shown, for a homogeneous solution, the optimization problem becomes single valued such that

$$H_{\phi} = \frac{\partial^2 \phi}{\partial u^2} = -2\beta \omega_0 + [1 - \tanh^2(\beta \epsilon)] \left(\frac{4\beta u}{\epsilon} \right)^2 + \beta \tanh(\beta \epsilon) \left(\frac{4}{\epsilon} - \frac{16u^2}{\epsilon^3} \right). \quad (\text{C10})$$

If we evaluate the Hessian at $\bar{u} = 0$, which is always a solution of Eq. (C9) we obtain

$$H_\phi(\bar{u} = 0) = -2\beta\omega_0 + \beta \tanh\left(\beta \frac{\omega_z}{2}\right) \frac{8}{\omega_z}, \quad (\text{C11})$$

which is always negative for $\Gamma < \omega_z/4$, i.e., for $\omega_0 = 1/\Gamma > 4/\omega_z$. For $\omega_0 > 4/\omega_z$, the sign depends on β , being negative for $\beta < \beta_c$ with $\omega_0\omega_z = 4 \tanh(\beta_c\omega_z/2)$. So in the regime where $\bar{u} = 0$ is the only solution to Eq. (C9), it is a maximum. For $\omega_0 < 4/\omega_z$ and $\beta > \beta_c$ a nontrivial solution given by $\omega_0\bar{\epsilon} = 2 \tanh(\beta\bar{\epsilon})$ appears and can be shown graphically to be the maximum. Therefore, Eq. (C9) always has a solution that is a maximum of ϕ .

3. Proof that the homogeneous solution is the global maximum

We cannot rule out the existence of inhomogeneous extrema of ϕ , i.e., inhomogeneous solutions of Eq. (C6). Instead, we show that if there exists an inhomogeneous solution and it is a maximum, it is a local maximum, with the global maximum given by the homogeneous solution.

Let us express the self-consistent condition for the extrema of ϕ given in Eq. (C6) in terms of $\{\mu_i\}$ and $\{\epsilon_i\}$:

$$\frac{1}{2N} \sum_i^N \lambda_{ik} \bar{\mu}_i \omega_k = \frac{1}{N} \sum_i^N \tanh(\beta\bar{\epsilon}_i) \frac{\lambda_{ik} \bar{\mu}_i}{\bar{\epsilon}_i}. \quad (\text{C12})$$

Isolating the $\{\bar{\mu}_i\}$ yields the self-consistent condition

$$\bar{\mu}_i = 2 \sum_j^N \tanh(\beta\bar{\epsilon}_j) \frac{\bar{\mu}_j}{\bar{\epsilon}_j} J_{ij}, \quad (\text{C13})$$

which is simply a reformulation of the maximization problem in terms of new variables. Accordingly, ϕ reads as

$$\phi[\mu_i] = -\frac{\beta}{4N} \sum_{ij}^N \mu_i J_{ij}^+ \mu_j + \frac{1}{N} \sum_i^N \ln [2 \cosh(\beta\epsilon_i)], \quad (\text{C14})$$

with $NJ_{ij}^+ = \sum_k \lambda_{ik} \omega_k \lambda_{jk}$. Note that $JJ^+J = J$. Substituting Eq. (C13) in (C14) yields

$$\begin{aligned} \phi[\bar{\mu}_i] &= -\frac{\beta}{2N} \sum_i^N \frac{\tanh(\beta\bar{\epsilon}_i)}{\bar{\epsilon}_i} \bar{\mu}_i^2 + \frac{1}{N} \sum_i^N \ln [2 \cosh(\beta\bar{\epsilon}_i)] \\ &= \frac{1}{N} \sum_i^N \xi(\bar{\mu}_i). \end{aligned} \quad (\text{C15})$$

We can particularize this expression for the homogeneous solution, $\bar{\mu}_i \equiv \bar{\mu}$,

$$\begin{aligned} \phi(\bar{\mu}) &= -\frac{\beta \tanh(\beta\bar{\epsilon})}{2} \frac{\bar{\mu}^2}{\bar{\epsilon}} + \ln [2 \cosh(\beta\bar{\epsilon})] \\ &= \frac{1}{N} \sum_i^N \xi(\bar{\mu}). \end{aligned} \quad (\text{C16})$$

Note that because $\bar{\mu}$ maximizes ϕ , it also maximizes ξ . Therefore, an inhomogeneous maximum of ϕ given by $\{\bar{\mu}_i\}$ cannot maximize ξ for all $\bar{\mu}_i$ (to the extent that some $\bar{\mu}_i$ must deviate from $\bar{\mu}$ in order for the configuration to be inhomogeneous) and thus $\phi(\bar{\mu}) \geq \phi[\bar{\mu}_i]$. The global maximum of ϕ is given by the homogeneous solution.

APPENDIX D: ANALYTICAL CALCULATION OF SUSCEPTIBILITIES

From Eqs. (20) and (C6) we realize that

$$\bar{u}_k \omega_k = \frac{1}{N} \sum_i^N \langle \sigma_i^x \rangle \lambda_{ik} \quad (\text{D1})$$

and thus

$$\frac{\partial \bar{u}_k}{\partial h_j} \omega_k = \frac{1}{N} \sum_i^N \chi_{ij} \lambda_{ik}. \quad (\text{D2})$$

From Eq. (19) we have

$$\chi_{ij} = \lim_{\{h_n\} \rightarrow 0} \left(2 \sum_{k=0}^{M-1} \lambda_{ik} \frac{\partial \bar{u}_k}{\partial h_j} + \delta_{ij} \right) Y_i, \quad (\text{D3})$$

with

$$\begin{aligned} Y_i &= (1 - \tanh^2(\beta\bar{\epsilon}_i)) \beta \left(\frac{\bar{\mu}_i + h_i}{\bar{\epsilon}_i} \right)^2 \\ &\quad + \tanh(\beta\bar{\epsilon}_i) \frac{1}{\bar{\epsilon}_i} \left[1 - \left(\frac{\bar{\mu}_i + h_i}{\bar{\epsilon}_i} \right)^2 \right]. \end{aligned} \quad (\text{D4})$$

From Eqs. (D2) and (D3) and after some manipulation, we find

$$\chi_{ij} = \left(2 \sum_r^N J_{ir} \chi_{rj} + \delta_{ij} \right) Y, \quad (\text{D5})$$

where $Y = \lim_{\{h_n\} \rightarrow 0} Y_i$. For a translation-invariant model, Eq. (D5) can be solved in Fourier space. We define

$$\chi_{ij} = \frac{1}{N} \sum_{k=0}^{N-1} \lambda_{ik} \chi_k \lambda_{jk} \quad (\text{D6})$$

and find

$$\chi_k = \frac{Y}{1 - 2YD_k}. \quad (\text{D7})$$

Here D_k are the eigenvalues of J [cf. Eq. (7)]. The susceptibilities in real space are thus given by

$$\begin{aligned} \chi_{ij} &= \frac{1}{N} \left(\sum_{k=0}^{M-1} \lambda_{ik} \chi_k \lambda_{jk} + Y \sum_{k=M}^{N-1} \lambda_{ik} \lambda_{jk} \right) \\ &= \frac{1}{N} \left[\sum_{k=0}^{M-1} \lambda_{ik} \chi_k \lambda_{jk} + Y \left(N \delta_{ij} - \sum_{k=0}^{M-1} \lambda_{ik} \lambda_{jk} \right) \right], \end{aligned} \quad (\text{D8})$$

leading to Eq. (22).

- [1] J. W. Britton, B. C. Sawyer, A. C. Keith, C.-C. J. Wang, J. K. Freericks, H. Uys, M. J. Biercuk, and J. J. Bollinger, Engineered two-dimensional ising interactions in a trapped-ion quantum simulator with hundreds of spins, *Nature (London)* **484**, 489 (2012).
- [2] M. Knap, A. Kantian, T. Giamarchi, I. Bloch, M. D. Lukin, and E. Demler, Probing real-space and time-resolved correlation functions with many-body ramsey interferometry, *Phys. Rev. Lett.* **111**, 147205 (2013).
- [3] C. Monroe, W. C. Campbell, L. M. Duan, Z. X. Gong, A. V. Gorshkov, P. W. Hess, R. Islam, K. Kim, N. M. Linke, G. Pagano, P. Richerme, C. Senko, and N. Y. Yao, Programmable quantum simulations of spin systems with trapped ions, *Rev. Mod. Phys.* **93**, 025001 (2021).
- [4] A. Browaeys and T. Lahaye, Many-body physics with individually controlled Rydberg atoms, *Nat. Phys.* **16**, 132 (2020).
- [5] D. Mukamel, Statistical mechanics of systems with long range interactions, in *AIP Conference Proceedings*, Volume 970 (AIP, Melville, NY, 2008), p. 22 [10.1063/1.2839123](https://doi.org/10.1063/1.2839123).
- [6] A. Campa, T. Dauxois, and S. Ruffo, Statistical mechanics and dynamics of solvable models with long-range interactions, *Phys. Rep.* **480**, 57 (2009).
- [7] S. Fey and K. P. Schmidt, Critical behavior of quantum magnets with long-range interactions in the thermodynamic limit, *Phys. Rev. B* **94**, 075156 (2016).
- [8] N. Defenu, T. Donner, T. Macrì, G. Pagano, S. Ruffo, and A. Trombettoni, Long-range interacting quantum systems, *Rev. Mod. Phys.* **95**, 035002 (2023).
- [9] N. Defenu, A. Leroise, and S. Pappalardi, Out-of-equilibrium dynamics of quantum many-body systems with long-range interactions, [arXiv:2307.04802](https://arxiv.org/abs/2307.04802).
- [10] T. Koffel, M. Lewenstein, and L. Tagliacozzo, Entanglement entropy for the long-range ising chain in a transverse field, *Phys. Rev. Lett.* **109**, 267203 (2012).
- [11] T. Kuwahara and K. Saito, Area law of noncritical ground states in 1d long-range interacting systems, *Nat. Commun.* **11**, 4478 (2020).
- [12] D. Vodola, L. Lepori, E. Ercolessi, A. V. Gorshkov, and G. Pupillo, Kitaev chains with long-range pairing, *Phys. Rev. Lett.* **113**, 156402 (2014).
- [13] F. Ares, J. G. Esteve, F. Falceto, and A. R. de Queiroz, Entanglement entropy in the long-range Kitaev chain, *Phys. Rev. A* **97**, 062301 (2018).
- [14] D. Vodola, L. Lepori, E. Ercolessi, and G. Pupillo, Long-range ising and Kitaev models: phases, correlations and edge modes, *New J. Phys.* **18**, 015001 (2015).
- [15] L. Vanderstraeten, M. VanDamme, H. P. Büchler, and F. Verstraete, Quasiparticles in quantum spin chains with long-range interactions, *Phys. Rev. Lett.* **121**, 090603 (2018).
- [16] G. Francica and L. Dell'Anna, Correlations, long-range entanglement, and dynamics in long-range Kitaev chains, *Phys. Rev. B* **106**, 155126 (2022).
- [17] J. T. Schneider, J. Despres, S. J. Thomson, L. Tagliacozzo, and L. Sanchez-Palencia, Spreading of correlations and entanglement in the long-range transverse ising chain, *Phys. Rev. Res.* **3**, L012022 (2021).
- [18] S. B. Jäger, L. Dell'Anna, and G. Morigi, Edge states of the long-range Kitaev chain: An analytical study, *Phys. Rev. B* **102**, 035152 (2020).
- [19] O. Viyuela, D. Vodola, G. Pupillo, and M. A. Martin-Delgado, Topological massive dirac edge modes and long-range superconducting hamiltonians, *Phys. Rev. B* **94**, 125121 (2016).
- [20] J. A. Koziol, A. Langheld, S. C. Kapfer, and K. P. Schmidt, Quantum-critical properties of the long-range transverse-field ising model from quantum monte carlo simulations, *Phys. Rev. B* **103**, 245135 (2021).
- [21] E. G. Lazo, M. Heyl, M. Dalmonte, and A. Angelone, Finite-temperature critical behavior of long-range quantum ising models, *SciPost Phys.* **11**, 076 (2021).
- [22] T. Mori, Equilibrium properties of quantum spin systems with nonadditive long-range interactions, *Phys. Rev. E* **86**, 021132 (2012).
- [23] A. Campa, A. Giansanti, and D. Moroni, Canonical solution of a system of long-range interacting rotators on a lattice, *Phys. Rev. E* **62**, 303 (2000).
- [24] T. Mori, Instability of the mean-field states and generalization of phase separation in long-range interacting systems, *Phys. Rev. E* **84**, 031128 (2011).
- [25] T. Mori, Analysis of the exactness of mean-field theory in long-range interacting systems, *Phys. Rev. E* **82**, 060103(R) (2010).
- [26] T. Mori, Microcanonical analysis of exactness of the mean-field theory in long-range interacting systems, *J. Stat. Phys.* **147**, 1020 (2012).
- [27] A. Campa, A. Giansanti, and D. Moroni, Canonical solution of classical magnetic models with long-range couplings, *J. Phys. A: Math. Gen.* **36**, 6897 (2003).
- [28] Y. K. Wang and F. T. Hioe, Phase transition in the Dicke model of superradiance, *Phys. Rev. A* **7**, 831 (1973).
- [29] F. T. Hioe, Phase transitions in some generalized Dicke models of superradiance, *Phys. Rev. A* **8**, 1440 (1973).
- [30] J. Román-Roche, F. Luis, and D. Zueco, Photon condensation and enhanced magnetism in cavity QED, *Phys. Rev. Lett.* **127**, 167201 (2021).
- [31] J. Román-Roche and D. Zueco, Effective theory for matter in non-perturbative cavity QED, *SciPost Phys. Lect. Notes* **50** (2022).
- [32] J. Simon, W. S. Bakr, R. Ma, M. E. Tai, P. M. Preiss, and M. Greiner, Quantum simulation of antiferromagnetic spin chains in an optical lattice, *Nature (London)* **472**, 307 (2011).
- [33] M. P. Kaicher, D. Vodola, and S. B. Jäger, Mean-field treatment of the long-range transverse field Ising model with fermionic Gaussian states, *Phys. Rev. B* **107**, 165144 (2023).
- [34] Z.-X. Gong, M. F. Maghrebi, A. Hu, M. L. Wall, M. Foss-Feig, and A. V. Gorshkov, Topological phases with long-range interactions, *Phys. Rev. B* **93**, 041102(R) (2016).
- [35] E. H. Lieb, The classical limit of quantum spin systems, *Commun. Math. Phys.* **31**, 327 (1973).
- [36] I. G. Brankov, V. A. Zagrebnov, and I. S. Tonchev, Asymptotically exact solution of the generalized Dicke model, *Theor. Math. Phys.* **22**, 13 (1975).
- [37] R. Gibberd, Equivalence of the Dicke maser model and the ising model at equilibrium, *Aust. J. Phys.* **27**, 241 (1974).
- [38] D. Sadhukhan and J. Dziarmaga, Is there a correlation length in a model with long-range interactions? [arXiv:2107.02508](https://arxiv.org/abs/2107.02508).
- [39] R. Kubo, M. Toda, and N. Hashitsume, *Statistical Physics II* (Springer, Berlin, 1991).
- [40] F. Schwabl, *Statistical Mechanics* (Springer, Berlin, 2006).

- [41] K. Hepp and E. H. Lieb, On the superradiant phase transition for molecules in a quantized radiation field: the Dicke maser model, *Ann. Phys.* **76**, 360 (1973).
- [42] K. Hepp and E. H. Lieb, Equilibrium statistical mechanics of matter interacting with the quantized radiation field, *Phys. Rev. A* **8**, 2517 (1973).
- [43] J. I. Latorre, R. Orús, E. Rico, and J. Vidal, Entanglement entropy in the Lipkin-Meshkov-Glick model, *Phys. Rev. A* **71**, 064101 (2005).